Focusing Inversion of Electroencephalography and Magnetoencephalography Data

Portniaguine O., Weinstein D., and Johnson C.

University of Utah, Salt Lake City, USA
email: {oleg|dmw|crj}@cs.utah.edu
URL: http://www.sci.utah.edu

Introduction

The inverse electroencephalography (EEG) and magnetoencephalography (MEG) problems seek to reconstruct neural sources based on measurements of the electric or magnetic field recorded outside of the head. In this paper, we present a new minimization technique for solving these problems. Our contribution is a novel stabilizing functional that is proven to have minimal support.

Motivation

Two neuroscience applications that stand to benefit from accurate solutions to the inverse bioelectric and biomagnetic field problems are functional brain studies and clinical diagnosis of neural disease, such as epilepsy. In functional brain studies, sensory signals stimulate the subject, and the brain's electromagnetic activity appears as a response to these stimuli. The signal is measured by a sensor array outside of the head. The location and strength of the neural sources that were activated due to the stimulus can, in theory, be determined by solving the inverse imaging problem [6–8].

As with functional studies, the neural activity of epileptic seizures can also be measured by sensors external to the head. Here again, accurately localizing the sources of the neural activity is a fundamental problem. Almost two million people in the U.S. suffer from epilepsy, a brain disease that can be described as an abnormal electrical function within the brain. However, only 20% of the epileptic surgical candidates can be diagnosed on the basis of non-invasive imaging alone, due to the current shortcomings of inverse imaging methods. The remaining candidates often require risky and expensive invasive procedures in order to localize the epileptogenic focus.

Methods

As with most inverse imaging problems, the inverse solution to the bioelectric and biomagnetic field problems are grossly under-determined. That is, there are many more possible neural source locations than there are sensors measurement sites. As a result, we require constraints for our solutions. An approach based on Tikhonov regularization [7] provides a common framework for bioelectric and biomagnetic inverse problems. The equation:

$$||\mathbf{LI} - \boldsymbol{\phi}||^2 + \lambda S(\mathbf{I}) = min, \qquad (1)$$

defines this approach, where $\mathbf{I}$ describes the model parameters that we seek to find, $\boldsymbol{\phi}$ represents the data, and $\mathbf{L}$ is the sensitivity (lead field) matrix. The stabilizing functional $S(\mathbf{I})$ encapsulates all additional information (or constraints) on the model parameters [1, 2]. Depending on the particular case, we can replace the abstract terms of "model" and "data" with specific quantities. For example, in the case of the inverse EEG problem, "data" are the electric potential measurements from the head surface, and "model" might be the distribution of current sources inside the head. For the inverse MEG problem, "data" are the measured magnetic field values, and "model" is the distribution of the current sources inside the head.

While simple to formulate, inverse problems present many challenges in implementation and in selecting an appropriate constraint $S(\mathbf{I})$, because the problem is inherently ill-posed. That is, the solution may not exist, may be non-unique, and may be unstable. Too loose of a constraint can lead to unbounded oscillations in the solution, while applying too tight of a constraint leads to overly smooth solutions that mask important details. The choice of constraint also depends on the problem. The focusing method that we present here is based on a specially selected minimum support constraint $S(\mathbf{I})$ [1, 2].

Focusing inversion provides a means of reconstructing sharp images from remotely measured, smoothed, or blurred data. Its origins lie in geophysics for two-dimensional gravitational inversion [2], while a more recent application is inverse MEG [1]. Portniaguine and Zhdanov [5] have formulated a new robust version of the algorithm as a minimization of a Tikhonov parametric functional that features a specially selected focusing stabilizer:

$$||\mathbf{LI} - \boldsymbol{\phi}||^2 + \lambda \sum_{i=1}^{N_i} \frac{f_i^2}{f_i^2 + \beta^2} = min, \qquad (2)$$

where $\mathbf{I}$ is the vector of model parameters, of length N_i; I_i is the i-th element of a model vector (strength of the dipole component for a corresponding voxel); $\mathbf{L}$ is the lead field (sensitivity) matrix; ϕ is the vector of observed data (electric potentials for EEG, magnetic fields for MEG); λ is the regularization parameter; and β is the damping parameter.

An efficient construction for the EEG lead field matrix was computed by Weinstein et al.,using the reciprocity theorem [8]. The lead field for the MEG problem was computed using locally fit conductive spheres by Sarvas [6].

For the numerical implementation of focusing inversion, we reformulate the problem in the space of weighted model parameters [5]. Eqn.(2) can be reformulated by splitting the stabilizer quotient into a product of two terms:

$$||\mathbf{LI} - \phi||^2 + \lambda \sum_{i=1}^{N_i} \frac{1}{I_i^2 + \beta^2} I_i^2 = min. \quad (3)$$

We introduce the iterative weights:

$$\mathbf{W}(\mathbf{I}) = diag(abs(\sqrt{\mathbf{I}^2 + \beta^2})). \quad (4)$$

When β is close to zero, this reduces to:

$$\mathbf{W}(\mathbf{f}) \approx diag(abs(\mathbf{I})), \quad (5)$$

where $\mathbf{W}(\mathbf{I})$ is a diagonal weighting matrix. Now, we can rewrite Eqn.(3) in matrix notation:

$$||\mathbf{LW}(\mathbf{I})\mathbf{W}(\mathbf{I})^{-1}\mathbf{I} - \phi||^2 + \lambda||\mathbf{W}(\mathbf{I})^{-1}\mathbf{I}||^2 = min. \quad (6)$$

We transform Eqn.(6) into a space of weighted model parameters $\mathbf{f}_w$ by replacing the variables:

$$\mathbf{L}_w = \mathbf{LW}(\mathbf{I}), \mathbf{I}_w = \mathbf{W}(\mathbf{I})^{-1}\mathbf{I}. \quad (7)$$

Substituting these expressions into Eqn.(6) yields

$$||\mathbf{L}_w\mathbf{I}_w - \phi||^2 + \lambda||\mathbf{I}_w||^2 = min. \quad (8)$$

Note that in Eqn.(6), the multiplier $\mathbf{W}(\mathbf{I})$ depends on $\mathbf{I}_w$. This equation can be solved using the reweighting algorithm, where a linear problem for $\mathbf{I}_w$ is solved in each step with fixed $\mathbf{W}$, using the conjugate gradient (CG) algorithm:

$$\begin{aligned} \mathbf{l}_i &= \mathbf{L_w}^T \mathbf{r}_{i-1} \\ s_i &= \mathbf{l}_i^T \mathbf{l}_i \\ \mathbf{h}_i &= \mathbf{l}_i + \mathbf{h}_{i-1} \tfrac{s_i}{s_{i-1}} \\ \mathbf{p}_i &= \mathbf{L_w} \mathbf{h}_i \\ k_i &= \tfrac{\mathbf{I}_i^T \mathbf{h}_i}{\mathbf{I}_i^T \mathbf{p}_i} \\ \mathbf{I}_{wi} &= \mathbf{I}_{wi-1} - k_i \mathbf{h}_i \\ \mathbf{r}_i &= \mathbf{r}_{i-1} - k_i \mathbf{p}_i, \end{aligned} \quad (9)$$

where i is the iteration number, $\mathbf{r}$ is the residual vector, $\mathbf{l}$ is the gradient vector, s is its length, $\mathbf{h}$ is the conjugate direction vector in the space of models, $\mathbf{p}$ is its projection in the space of data, and k is the step length, a scalar. After generating the CG solution, $\mathbf{I}$ is updated using (7) and $\mathbf{W}(\mathbf{I})$ is updated using (5).

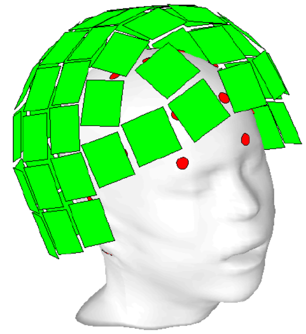

Figure 1: A patient with electroencephalography (EEG) electrodes on the head and MEG sensors corresponding to the measuring helmet. From two dipoles placed on the cortical surface, we have simulated MEG response.

A number of researchers have investigated the convergence and other properties of reweighted optimization [3, 10]. Last and Kubic [2] used reweighting in Eqn.(3), where the weights were left in the stabilizer. This lead to implementation difficulties, such as the necessity to choose the parameter β, which is non-trivial since for very small values of β the problem has singularities when the individual parameters m_i are close to zero. Our method is based on Eqn.(8), and is similar to that of Gorodnitsky and Rao [1]. In [1] they found empirically that the reweighting lead to focusing of the image. In contrast, our derivation is rigorous, as it is based on the minimization of a parametric functional (2).

Results

We will now demonstrate the application of focusing inversion to the EEG and MEG inverse problems. Two dipoles were placed in a model created from a patient's head MRI to represent a simplified neural source. We then divided the volume of the brain into voxels and simulated the resulting electric and magnetic field values at the sensor sites. Finally, we constructed the EEG and MEG lead fields, and used focusing inversion to recover the magnitudes of the three dipole components in each voxel. Using our technique, we were able to localize the dipoles within 3 mm of their true positions for the MEG problem and 9 mm for EEG.

Fig. 1 shows a patient with EEG electrodes on their head and MEG sensors corresponding to the measuring helmet. Fig. 2 shows the reconstruction of the locations of the dipoles using focusing inversion (yellow isolines surround the predicted dipole locations, while red stars show the true locations of the dipoles). Fig. 3 shows a rendering of a slice in the geometric model that contains the dipole locations, superimposed on a wire mesh of the head. The volume of the head was represented by 8000 voxels.

For the EEG solution, we constructed a finite element mesh with five conductivity classifications and

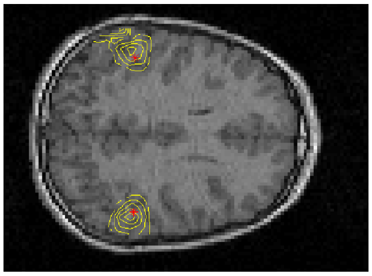

Figure 2: Reconstruction of the locations of the dipoles using focusing inversion. Yellow isolines surround predicted dipole locations, while stars show true location of the dipoles.

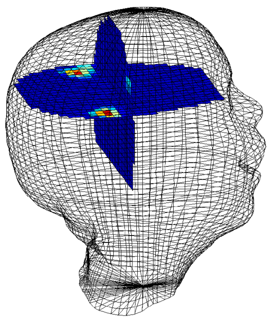

Figure 3: Rendering of slices containing the dipole locations in the geometric model, superimposed on a wire mesh of the head.

396,285 tetrahedral elements. The geometric model included 129 electrode recording sites on the scalp surface. An image of the mesh and electrodes is shown in Fig. 4. Following the reciprocity-based algorithm described in [8], we proceeded to construct the element-based lead field for the model. We then generated the forward EEG solution at the electrodes for two simulated dipoles placed within the cortex, as described in [9]. Finally, we ran focusing inversion to recover activated areas of the head model. The algorithm succeeded in localizing the dipole sources with an accuracy of 9 mm, as shown in Fig. 5.

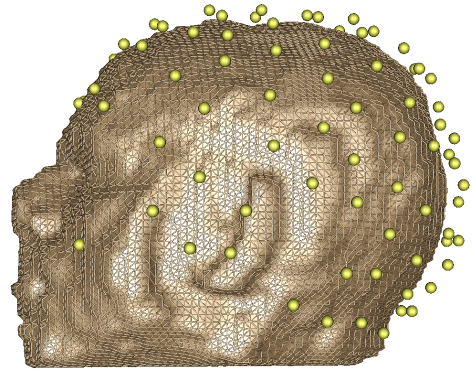

Figure 4: The boundary of the finite element mesh and the electrode recording sites used for the inverse EEG simulations.

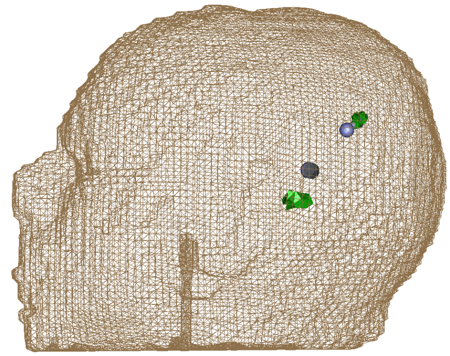

Figure 5: Isosurface of the focused inversion solution, shown with the actual dipole sources. Solution accuracy is 9 mm.

References

[1] Gorodnitsky, I.F., and Rao, B.D. Sparse signal reconstruction from limited data using FOCUSS: A recursive Weighted Norm Minimization Algorithm, IEEE Trans. on Signal Processing, 45:600-616, 1997.

[2] Last, B. J., and Kubik, K. Compact gravity inversion, Geophysics, 48:713-721, 1983.

[3] O'Leary, D.P., Robust regression computation using iteratively reweighted least squares, SIAM J. Matrix Anal. Appl., 11:466-480, 1990.

[4] Portniaguine, O. Image focusing and data compression in the solution of geophysical inverse problems, Ph.D. dissertation, Univ. of Utah, 1999.

[5] Portniaguine, O., and Zhdanov, M.S. Focusing geophysical inversion images, Geophysics, 64:874-887, 1999.

[6] Sarvas, J. Basic mathematical and electromagnetic concepts of the biomagnetic inverse problem, Phys. Med. Biol., 32:11-22, 1987.

[7] Tikhonov, A.N., and Arsenin, Y.V. Solution of ill-posed problems, Winston and Sons, 1977.

[8] Weinstein, D., Zhukov, L., and Johnson, C. Lead-field bases for electroencephalography source imaging, Ann. Biomed. Eng., 28:1-7, 2000.

[9] Weinstein, D., Portniaguine, O., Zhukov, L. A Comparison of Dipolar and Focused Inversion for EEG Source Imaging, NFSI 2001.

[10] Wolke, R., and Schwetlick, H., Iteratively reweighted least squares: algorithms, convergence analysis, and numerical comparisons, SIAM J. Sci. Stat. Comput., 9:907-921, 1988.

Acknowledgments

This work was supported by the National Institutes of Health, National Center for Research Resources, grant number 1-P41-RR12553-2.